

Pedestal properties of mitigated ELMy H-modes at high density at ASDEX Upgrade

E. Wolfrum¹, M. Wiesinger², L. Barrera Orte¹, M. Bernert¹, M.G. Dunne¹, R. Fischer¹, S. Potzel¹, P.A. Schneider¹, W. Suttrop¹ and the ASDEX Upgrade Team

¹ Max-Planck-Institut für Plasmaphysik, Garching, Germany

² Institute for Applied Physics, Vienna University of Technology, Vienna, Austria

The application of magnetic perturbations (MP) via coils mounted inside the vessel can lead to mitigated ELMs. At ASDEX Upgrade mitigation of ELMs is reliably achieved at high line averaged electron densities in the pedestal ($\bar{n}_e > 0.65 \text{ n}_{\text{GW}}$) [1,2]. Without MPs, however, small ELMs also appear with sufficient fuelling. In this work the pedestal top properties of discharges featuring mitigated ELMs with and without application of MPs are compared. It will be shown that the pedestal top conditions, at which the small, mitigated ELMs appear, are the same with and without the application of MP coils. In addition, high power discharges with mitigated ELMs are analysed.

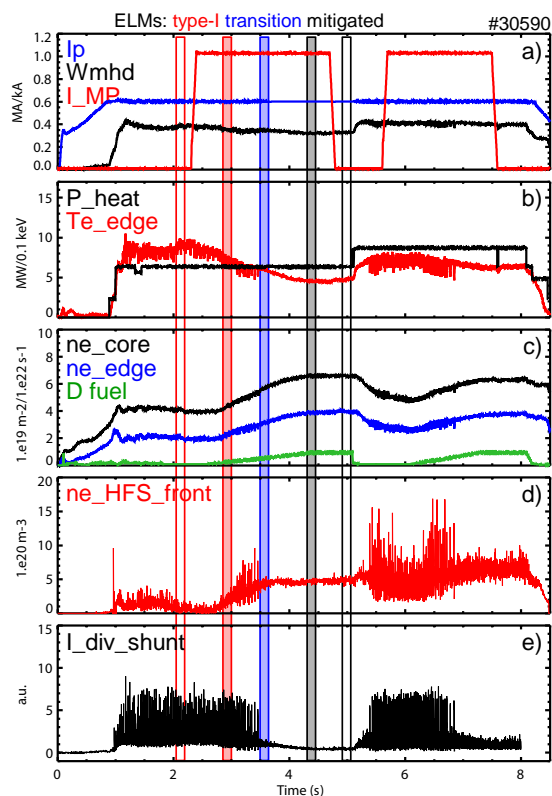


Figure 1: Time traces of #30590. a) Plasma current I_p , stored energy W_{mhd} , MP coil current, b) total heating power P_{heat} , edge temperature from ECE, c) core (H-0) and edge (H-5) line integrated density and D fuelling level, d) density in HFS n_e front, e) divertor current as ELM indicator.

The database presented in this work consists of around 200 time points which are separated into three categories: (i) before mitigation, i.e. with type-I ELMs (red), (ii) just after the last type-I ELM (blue) and (iii) well into the mitigated regime (black). Figure 1 displays time traces of an example discharge with two density ramps at different heating powers. It can clearly be seen, that ELMs are not immediately mitigated when MP coils are turned on. In this case this is due to the low density. Moreover, ELMs remain mitigated even after MP coils are switched off. The coloured bars denote the times for the determination of the pedestal top electron densities ($n_{e,\text{ped}}$) and temperatures ($T_{e,\text{ped}}$) via a two-line fit [3]. Data points with relative errors on $T_{e,\text{ped}}$ and $n_{e,\text{ped}}$ greater than 20% and 5%, respectively, have been discarded.

Figure 2 shows $n_{e,ped}$ vs. $T_{e,ped}$ for a) with MP coils, b) without MP coils and c) both together for three plasma currents. As can be seen, the mitigated phases (black and blue) are clustered at low temperatures and high densities. A separate analysis of the data at each plasma current shows that the kinetic parameters do not lie on lines of constant pressure at the onset of mitigation. The peeling-ballooning mode is therefore not the dominant mechanism.

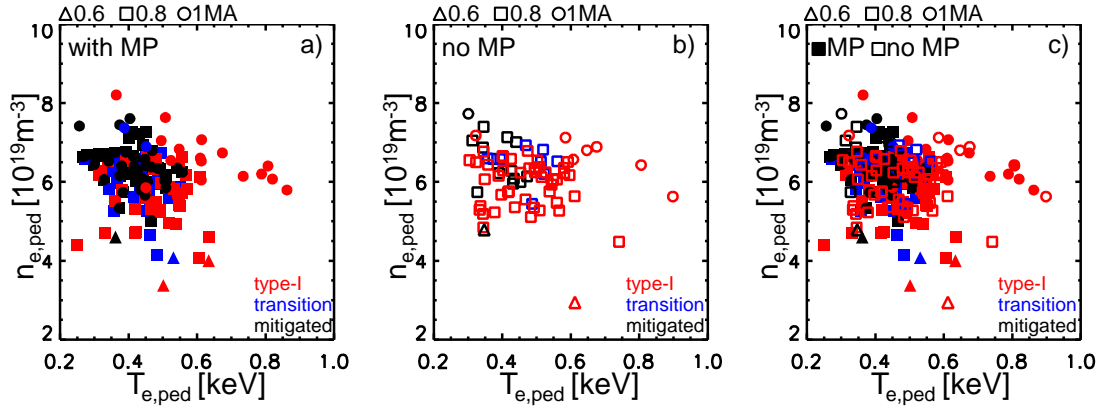


Figure 2: $n_{e,ped}$ vs. $T_{e,ped}$ for type-I ELMs (red), transition to mitigated ELMs (blue) and mitigated ELMs (black) for a) with MP coils (filled symbols), b) without MP coils (open symbols) and c) both together. Circles denote $I_p=1\text{MA}$, squares $I_p=0.8\text{ MA}$ and triangles $I_p=0.6\text{ MA}$.

The same data are displayed in figure 3 in terms of the dimensionless quantities neoclassical collisionality [4] ($Z_{eff}=1$) and Greenwald fraction of the density, again separately for with and without MP as well as combined.

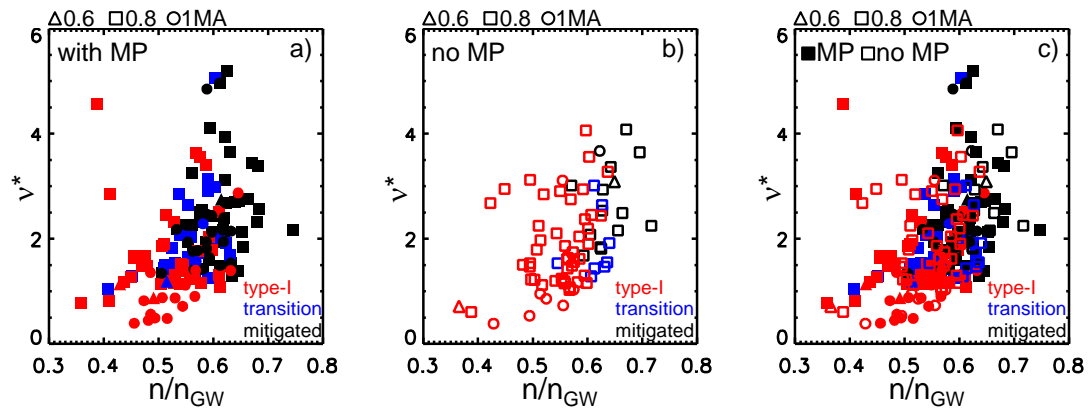


Figure 3: Collisionality versus Greenwald density fraction. Notation is the same as in figure 2.

The main finding is that the pedestal top values of electron density and electron temperature or the normalized parameters collisionality and Greenwald fraction do not show any systematic differences between cases with and without MP. Analysis of these pedestal top parameters separately did not yield a distinct threshold for the onset of mitigation. However, mitigation was found in most cases only at electron densities larger than $0.5 \cdot n_{GW}$, electron temperatures lower than 0.55 keV and collisionalities v^* larger than 1.2. There are very few examples with $T_{e,ped}$ less than 300 eV. These are very weakly heated discharges which show small ELMs below $0.5 \cdot n_{GW}$ with a collisionality above 1.2 despite the low density.

In an effort to demonstrate that type-I ELMs return as soon as the pedestal top temperature is raised above 0.55 keV dedicated experiments were carried out, in which the heating power was raised to a maximum value allowed in ASDEX Upgrade without radiative divertor cooling.

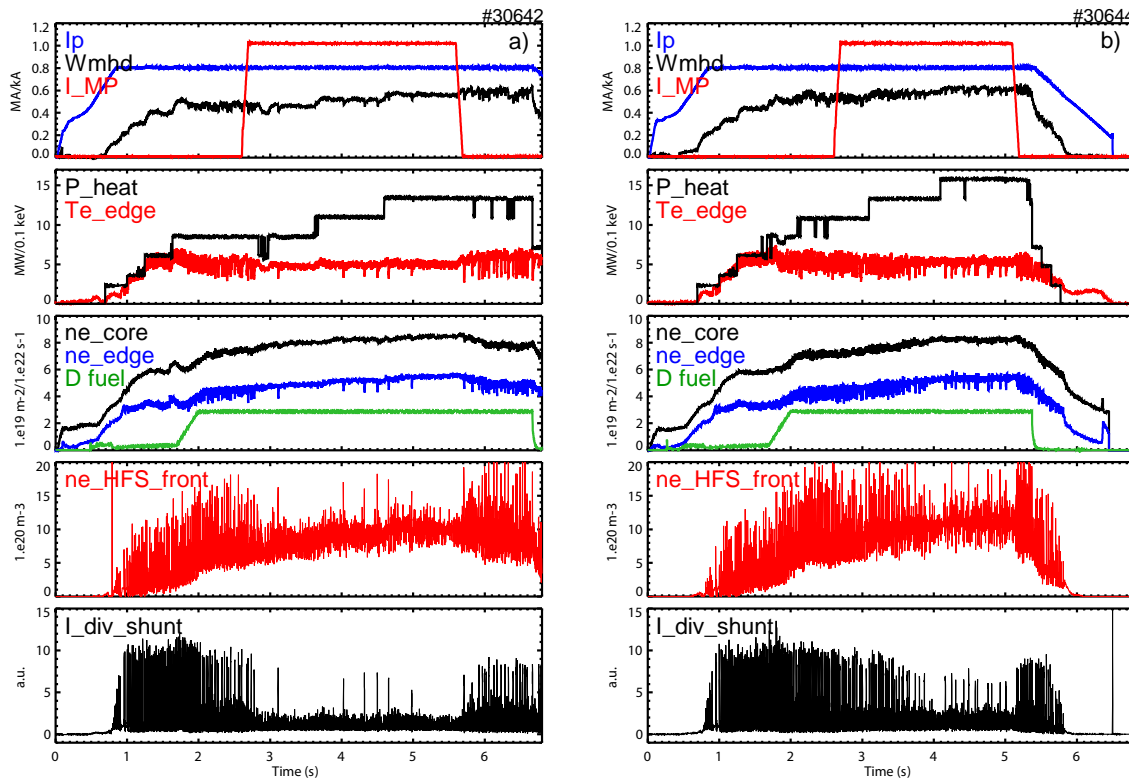


Figure 4: Time traces for #30642 and #30644. Notation same as in figure 1.

Figure 4 displays time traces of two discharges in which ELM mitigation is achieved at various levels of heating power. Note that in both discharges the gas fuelling has been kept constant. In discharge #30642 (Fig. 4a) mitigation is achieved for all three heating power levels (8.2, 10.8 and 13.2 MW). In discharge #30644 (Fig. 4b) partial mitigation is achieved at the two highest heating power levels (13.4 and 15.7 MW). In the latter discharge $T_{e,ped}$ is higher when the MP coils are turned on and a higher $n_{e,ped}$ is necessary to achieve mitigation, which is consistent with a threshold in collisionality. In both discharges, each step of heating power does not result in an increase of the pedestal top temperature, but causes an increase of the density. Under these conditions, the inner divertor is partially detached and a high density region is observed in the scrape-off layer (SOL) at the high field side at the height of the X-point expanding well above the X-point [5], which we will call HFS n_e front in the following. A possible cause for the observed density increase could be the interaction of MP induced magnetic field perturbations in the SOL and the HFS n_e front [6]. The density measured in the HFS n_e front is of the order of $\sim 10^{21} \text{ m}^{-3}$. With each step of heating power, the size of the HFS n_e front increases. A density increase is only possible if neutrals are ionized, suggesting that the electron temperature is above $\sim 10 \text{ eV}$. This results in a pressure gradient along a field line connecting the HFS n_e front with the separatrix ($n_{e,sep} \sim 2 \cdot 10^{19} \text{ m}^{-3}$, $T_{e,sep} \sim 100 \text{ eV}$) due to the magnetic field perturbation.

Figure 5 shows pedestal profiles of electron density and temperature at three time points of discharge #30644: a) at 2.4 s when MP coils are still off, b) at 2.88 s when MP coils are on, the heating power is the same (10.8 MW) and mitigation does not occur and c) at 4.65 s when MP coils are on, the heating power has been raised to 15.7 MW and ELMs are (not completely) mitigated. Although the heating power is significant, the pedestal top temperatures never exceed 0.6 keV.

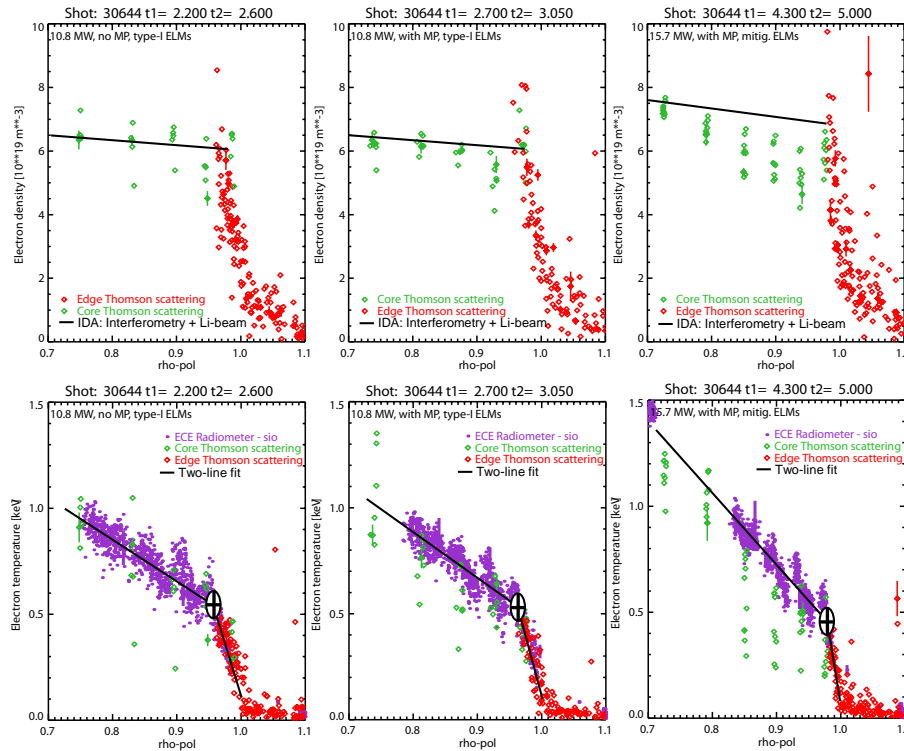


Figure 5: Top row: Edge electron density profiles from core (green) and edge (red) Thomson scattering as well as from IDA(=interferometry+Li-beam), bottom row: edge electron temperature profiles from TS and ECE (purple).

The outer channels of the core Thomson scattering (TS) diagnostic [7] show significantly lower values than the measurements at the midplane (edge TS, ECE, IDA from interferometry and Li-beam). As these outer TS channels are located halfway between the mid-plane and the X-point, the MP induced perturbations of the magnetic field could cause a connection to the wall and thus locally decrease T_e and n_e .

In summary, it has been shown that there is no difference in the pedestal properties of mitigated ELMs with and without MPs. The increase in density, which is observed after applying MPs, is even more pronounced at high heating power. An explanation could be the following: the MP induced lobes of the magnetic field connect the confined plasma on the LFS to the wall and on the HFS to the HFS n_e front, changing the balance between SOL layer and confined plasma.

This project has received funding from the Euratom research and training programme 2014-2018.

References:

- 1 W. Suttrop et al., PRL 106 (2011) 225004
- 2 R. Fischer et al., PPCF 54 (2012) 115008
- 3 P. A. Schneider et al., 54 (2012) 105009
- 4 O. Sauter et al, Phys. Plasmas 6 (1999) 2834
- 5 S. Potzel et al., NF 54 (2014) 013001
- 6 E. Wolfrum et al., EPS 2013, Helsinki
- 7 B. Kurzan et al., RSI 82 (2011)103510